VU Research Portal

A stringent limit on a drifting proton-to-electron mass ratio from alcohol in the early Universe

Bagdonaite, J.; Jansen, P.; Henkel, C.; Bethlem, H.L.; Menten, K.; Ubachs, W.M.G.

document version
Publisher's PDF, also known as Version of record

Link to publication in VU Research Portal

A Stringent Limit on a Drifting Proton-to-Electron Mass Ratio from Alcohol in the Early Universe

Julija Bagdonaite,[1] Paul Jansen,[1] Christian Henkel,[2,3] Hendrick L. Bethlem,[1] Karl M. Menten,[2] Wim Ubachs[1]*

The standard model of physics is built on the fundamental constants of nature, but it does not provide an explanation for their values, nor require their constancy over space and time. Here we set a limit on a possible cosmological variation of the proton-to-electron mass ratio μ by comparing transitions in methanol observed in the early universe with those measured in the laboratory. From radio-astronomical observations of PKS1830−211, we deduced a constraint of $\Delta\mu/\mu = (0.0 \pm 1.0) \times 10^{-7}$ at redshift $z = 0.89$, corresponding to a look-back time of 7 billion years. This is consistent with a null result.

The standard model of particle physics, the theory describing symmetries and forces of nature at the deepest level, does not provide an intrinsic explanation for the values of the fundamental coupling constants, nor does it prohibit that the fundamental constants depend on time and space. In contrast, Einstein's equivalence principle, a basic assumption of general relativity, assumes that the laws of nature, and hence the fundamental constants are independent of a local reference system. Some cosmological scenarios aimed at explaining the fine-tuning between fundamental constants sketch an evolving mechanism, where minimally varying constants are crucial for reaching the present state of complexity in the universe (1). Theoretical approaches involving additional scalar fields have imposed bounds on varying constants through tests of the weak equivalence principle (2). In the past decade the search for small variations of dimensionless fundamental constants over cosmological time scales has become an active experimental endeavor, in particular because accurate measurements of spectral lines of atoms at high redshift have provided indication for a possible variation of the fine structure constant α, either temporally (3, 4) or spatially (5, 6).

A second dimensionless fundamental constant μ, representing the proton-to-electron mass ratio m_p/m_e, probes the cosmological evolution of the nuclear versus the electroweak sector in the standard model. A search for a possible drift of μ has been made operational by comparing observations of spectral lines of the hydrogen molecule (H_2) in distant galaxies with accurate laboratory measurements (7). These investigations, based on

observations with the world's largest optical telescopes, have yielded a limit at the level of $\Delta\mu/\mu < 10^{-5}$ for look-back times of 12 billion years (8, 9).

Inversion transitions of ammonia (NH_3) were found to be ~100 times more sensitive to μ-variation than H_2 transitions (10, 11). Astronomical observations of NH_3, in the microwave or radio range of the electromagnetic spectrum, led to stringent 1σ constraints at the level of $(1.0 \pm 4.7) \times 10^{-7}$ (12) and $(-3.5 \pm 1.2) \times 10^{-7}$ (13). This has shifted the paradigm for probing μ-variation from optical

to radio astronomy. Here we use the extreme sensitivity of methanol (CH_3OH) (14, 15) to probe the variation of the proton-to-electron mass ratio μ over cosmic time.

Methanol (Fig. 1A) is the simplest alcohol and consists of a hydroxyl group attached to a methyl group. The C-O bond is flexible, allowing the hydroxyl group to rotate with respect to the methyl group. This so-called internal rotation is strongly hindered by the repulsion between the hydrogen atoms of the different groups, resulting in a threefold barrier (Fig. 1B). If the barrier were infinitely high, the levels in the torsional well would be degenerate. Quantum mechanical tunneling through the barriers lifts this degeneracy, resulting in three levels that are labeled according to symmetry: A, E1, and E2 (16). Because the symmetry of the nuclear wave function is preserved in radiative transitions as well as in (nonreactive) collisions, the A and E levels of methanol can be regarded as belonging to two separate chemical species

The sensitivity coefficient, K_μ, of a transition with frequency ν is defined by $\Delta\nu/\nu = K_\mu \times \Delta\mu/\mu$. The frequencies of pure rotational transitions, such as the transitions indicated by the red and orange arrow in Fig. 1C, are inversely proportional to the reduced mass of methanol and hence to the proton-to-electron mass ratio. Consequently, these have sensitivity coefficients equal to −1. The frequencies of pure torsional transitions— which are not allowed in methanol—depend exponentially on the reduced moments of inertia of

Fig. 1. (**A**) Pictorial representation of the methanol molecule. (**B**) Potential energy as a function of the dihedral angle between the OH group and one of the CH bonds in the methyl group. V_3 denotes the barrier height. The horizontal lines represent the energy for the levels in the torsion-vibrational ground state, $\nu_t = 0$, and first excited state, $\nu_t = 1$. (**C**) Energy level structure of the torsion-rotation ground state of methanol. Each level is labeled according to its torsional symmetry Ts, total angular momentum J, and its projection K on the molecule-fixed axis. The energy-level structure of methanol resembles that of a prolate symmetric top,
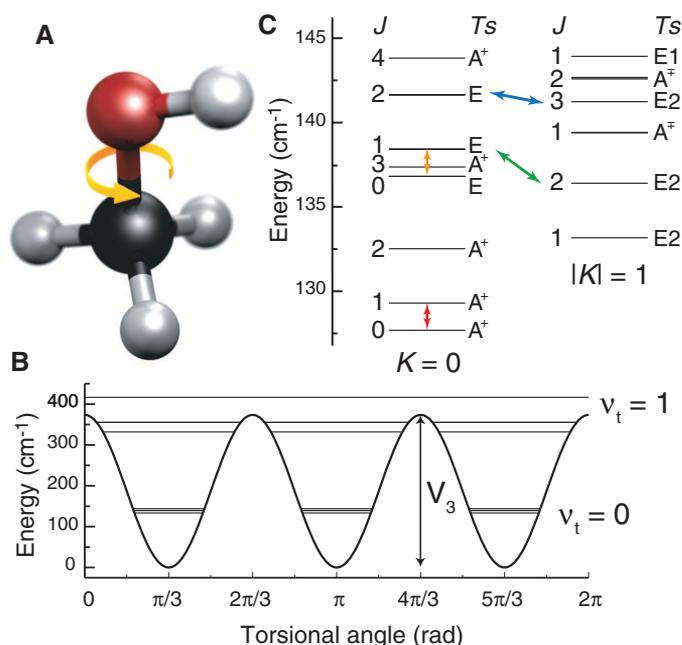
with the difference that each K manifold is offset depending on its torsional symmetry. Levels of A-symmetry with $|K| > 0$ are split by the slight asymmetry of the molecule. Levels of E1 and E2 symmetry in the $K = 0$ manifold cannot be distinguished and are labeled as E. The four transitions observed in this study are indicated by the four arrows. The transitions indicated by the red and orange arrows are pure rotational transitions and have a sensitivity coefficient of −1. The transitions indicated by the blue and green arrows are mixed torsion-rotation transitions and have sensitivity coefficients of −32.8 and −7.4, respectively.

[1]Department of Physics and Astronomy, VU University Amsterdam, De Boelelaan 1081, 1081 HV Amsterdam, Netherlands. [2]Max-Planck-Institut für Radioastronomie, Auf dem Hügel 69, 53121 Bonn, Germany. [3]Astronomy Department, King Abdulaziz University, Post Office Box 80203, Jeddah, Saudi Arabia.

*To whom correspondence should be addressed. E-mail: w.m.g.ubachs@vu.nl

the methyl and hydroxyl groups and have a sensitivity coefficient of –2.5. The sensitivity of mixed transitions—i.e., transitions in which both the internal and overall rotation state is changed—is strongly enhanced. The sensitivity coefficients for different transitions in methanol range from –42 to +53. These enhancements occur generally in every internal rotor molecule, but because of a number of favorable properties, the effect is exceptionally large in methanol (17).

Methanol is abundantly present in the universe, and more than a 1000 lines have been recorded in our galaxy (18). So far, searches for methanol absorption in far-distant galaxies have yielded detection only in the gravitational lens system PKS1830-211 (19). A limit on $\Delta\mu/\mu$ (20) has been previously derived on the basis of two methanol lines. We present a comprehensive study of radio astronomical observations of four methanol lines in PKS1830-211, including the two previously observed, with improved signal-to-noise ratio.

The background source of this system, PKS1830-211, is a high redshift ($z = 2.507$) blazar, which is radio loud and time variable and is viewed as two spotlike features and an Einstein ring, which result from gravitational lensing by the intervening face-on spiral galaxy (21, 22). The redshift of the main molecular absorptions from the galaxy is $z = 0.88582$ (19, 23), corresponding to a look-back time of 7.0 billion years, or half the age of the universe (24). More than 30 different molecular species were detected in the lensing galaxy of PKS1830-211 (19). Molecular absorption is mostly detected toward one of the two blazar images (the southwestern), whereas the other image (the northeastern) shows weaker and fewer molecular lines at a slightly different redshift but stronger neutral hydrogen absorption [e.g., (19, 25)].

The CH_3OH lines were recorded with the 100-m single-dish Effelsberg radio telescope, using the 5-, 1.3-, and 1-cm receivers. Preliminary detections were performed during the course of 2011, and subsequently systematic observations were performed in a narrow time slot. The data were registered onto a local standard of rest velocity scale, which was centered at $z = 0.88582$. The two blazar images and the Einstein ring are unresolved and PKS1830-211 is effectively treated as a point source, which is an assumption underlying the present study.

The recorded spectra are shown in Fig. 2. For a single transition, the spectra taken on various days were averaged together, weighting the individual scans by their integration time. The lines were calibrated by the total continuum so that their strength is expressed as line-to-continuum flux density ratio. The profiles, devoid of underlying structure, were fitted as a single Gaussian (Table 1). The accuracy of the position measurements is at the level of 1 to 4% of the line width. The velocities between different transitions are interrelated via

$$V/c = -K_\mu \Delta\mu/\mu$$

where c is the speed of light, and $\Delta\mu/\mu$ represents the deviation from the current laboratory value of μ, defined so that a positive sign indicates a larger μ in the high-redshift–absorbing

Fig. 2. Methanol absorption lines on a local standard of rest (LSR) velocity scale relative to $z = 0.88582$, observed toward PKS1830-211. The transitions and their approximate observed frequencies are indicated in each panel. The coloring of corresponding transitions matches that of Fig. 1. The top spectrum in each panel is a time-weighted average of the individual spectra, which are displayed below the combined one. For each spectrum, the position of a fitted Gaussian (depicted as light green curves) is shown in the graph at the right. Residuals are shown at the top of each combined spectrum with dashed lines indicating $\pm 1\sigma$ offsets. In the case of ~25-GHz observations, two proximate methanol transitions were recorded. They are separated by 27.494 km/s; the fitted positions of the weaker line are corrected to bring the measurements on a common scale. The lines are calibrated by the total continuum. The black square (upper panel) and the black diamond (lower panel) represent the single line observations from Ellingsen et al. (20) and Muller et al. (19), respectively. The line positions, originally reported on a heliocentric velocity scale, were transformed to the LSR scale via $V_{LSR} - V_{HEL} = 12.432$ km/s.
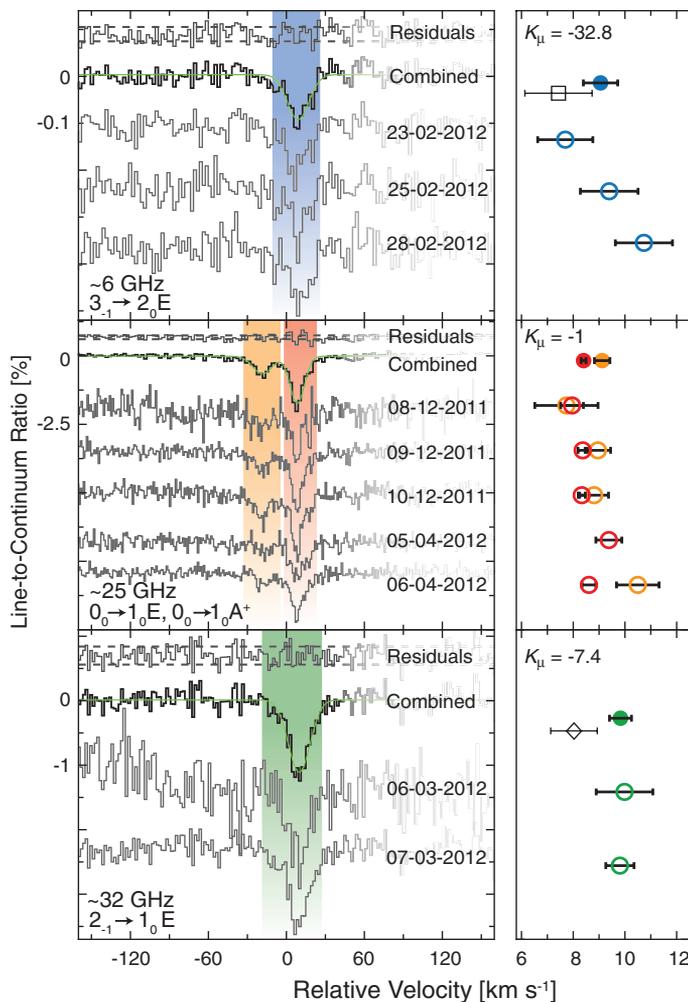
Table 1. A summary of the relevant parameters and results. Laboratory data: lower and upper energy level quantum numbers; laboratory frequencies, ν, of the four relevant methanol absorption lines; and their uncertainties, fractional uncertainties, and uncertainties in terms of Doppler shift, Δv_D, in km/s. Calculations: the sensitivity coefficients, K_μ. Observations: the measured local standard of rest velocities of the lines (relative to $z = 0.88582$) and the line widths with their 1σ uncertainties. Assuming a molecular hydrogen density of 2×10^3 cm^{-3} and a kinetic temperature of 80 K (12, 29), full width at half maximum linewidths as fitted to observations and a $T_{CMB} = 2.728(1 + z) = 5.145$ K for the temperature of the cosmic microwave background (CMB) radiation at $z = 0.88582$, the optical depths τ yield a total column density of 2.0×10^{14} cm^{-2} from a large velocity gradient radiative transfer model (30).

Line $J''_{K''}$–$J'_{K'}$ Ts	ν (GHz)	Δν/ν	Δv_D (km/s)	Ref.	K_μ	Position (km/s)	Width (km/s)	τ
3_{-1}–2_0 E	12.178597 (4)	3×10^{-7}	0.1	(31)	–32.8	9.06 ± 0.67	16.4 ± 1.4	0.0024
0_0–1_0 A$^+$	48.3724558 (7)	2×10^{-8}	0.006	(32)	–1	8.40 ± 0.10	10.8 ± 0.2	0.045
0_0–1_0 E	48.376892 (10)	2×10^{-7}	0.06	(33)	–1	9.12 ± 0.30	14.6 ± 0.6	0.016
2_{-1}–1_0 E	60.531489 (10)	2×10^{-7}	0.06	(33)	–7.4	9.83 ± 0.43	17.0 ± 0.9	0.028

Fig. 3. The positions of the four observed methanol lines (represented by V/c with respect to $z = 0.88582$) are plotted versus their sensitivity coefficients, K_μ. The bold blue horizontal line represents the fiducial result of a fit to the E-type lines, whereas the dashed line represents a fit to all four lines. A positive slope of the fitted line implies that μ had a smaller value in the early universe than is measured in the laboratory. The blue-shaded surface is a density plot of simulated data points from the blue fitted line and reflects the confidence bands of the fit. Color-coding of the data points is the same as in Figs. 1 and 2.
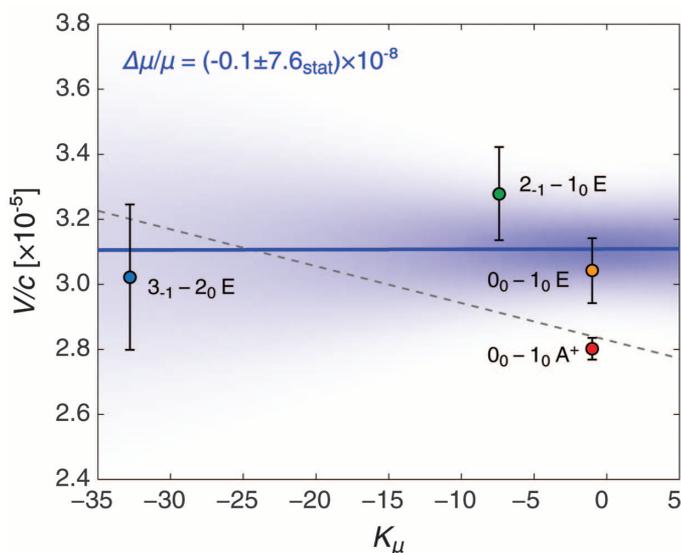
galaxy (i.e., $\Delta\mu = \mu_z - \mu_{lab}$). Therefore, to determine the fractional change in μ, the peak positions of the four transitions are plotted (in V/c) versus K_μ, and a (dashed) line is fitted to the data (Fig. 3). Because the A and E levels of methanol can be regarded as belonging to two separate species, the data were analyzed in two different ways: First, only the three transitions from E levels were fitted, then the A transition was added to the sample. The analysis of the E transitions results in $\Delta\mu/\mu = (-0.1 \pm 7.6) \times 10^{-8}$, which is consistent with a nonvarying μ at the level of 1.5×10^{-7} (95% confidence level). The reduced chi-squared, χ_ν^2, which is a measure of the quality of the fit, is ~2.0 (26). The fit on all four transitions has a much larger χ_ν^2 of 6.4, which might be attributed to segregation issues (see below), and it delivers $\Delta\mu/\mu = (11.0 \pm 6.8) \times 10^{-8}$.

The upper limit derived here is statistically more constraining than that derived in previous tests in the radio-domain (11–13, 19, 20). Moreover, compared to the methods used in previous studies, the methanol method is more robust against systematic effects. In particular, it is much less sensitive to the assumption that all absorbing species reside in the same physical location and hence are at the same redshift. Spatial segregation of different absorbers may mimic or hide a variation of μ. This is the limiting systematic error for tests based on the comparison between different molecular species, such as the comparison of ammonia with various rotational lines in HCO^+, HCN, CS, and so forth (11–13). The molecular survey in PKS1830-211 suggests that segregation effects are prominent among different species (19). For instance, a single methanol line was found to be displaced from the average absorption velocity by more than 3 km/s (19). Our test is based exclusively on a single molecular species. However, as discussed above, the E and

A type methanol should be considered as different species and thus may undergo spatial segregation effects. In the combined spectrum, the 0_0–1_0 A^+ and 0_0–1_0 E transitions, falling in close proximity in a single scan of the receiver, are separated by 0.72 ± 0.32 km/s. Moreover, the linewidths of the E lines are markedly larger than that of the A line (Table 1). Because this is suggestive of a spatial segregation of the E and A symmetry methanol molecules, we adopt a fiducial limit on $\Delta\mu/\mu$ from the fit of only E transitions.

Another source of systematic error is the known variability of the lensed object PKS1830-211. The absorption strength of radio lines was found to vary strongly, by a factor of >6 in a time span of 3 years, and this was ascribed to the intensity changes in the background continuum source (27). This phenomenon might cause a varying alignment through parts of the absorbing spiral and therewith absorption through varying Doppler components over time. Hence this variability may affect the derivation of a μ-constraint from radio-observations. For this reason we adopted a measurement strategy to explicitly address the source variability issue. Spectra of the anchor lines (the middle panel in Fig. 2) were recorded in December 2011 and April 2012, whereas the two strongly shifting lines have been observed in-between in February and March 2012 (28). The strong (0_0–1_0 A^+) line in the combined spectrum from December 2011 is positioned at 8.32 ± 0.10 km/s, and at 8.80 ± 0.24 km/s in the spectrum from April 2012. The difference between them is 0.48 ± 0.26 km/s, possibly indicative of a small systematic shift due to variability. We have assessed this possible systematic effect as caused by time variability in two models (26) and have chosen the one producing the largest uncertainty ($\Delta\mu/\mu$ of 7.0×10^{-8}) to give a conservative estimate.

Thus, we obtain a limit on varying μ to be $\Delta\mu/\mu = (-0.1 \pm 7.6_{stat} \pm 7.0_{sys}) \times 10^{-8}$ or, if the statistical and systematic uncertainties are added in quadrature, a limit of $\Delta\mu/\mu = (0.0 \pm 1.0) \times 10^{-7}$.

References and Notes

1. L. Smolin, *Physica A* **340**, 705 (2004).
2. J. D. Barrow, J. Magueijo, *Phys. Rev. D Part. Fields Gravit. Cosmol.* **72**, 043521 (2005).
3. J. K. Webb, V. V. Flambaum, C. W. Churchill, M. J. Drinkwater, J. D. Barrow, *Phys. Rev. Lett.* **82**, 884 (1999).
4. M. T. Murphy, J. K. Webb, V. V. Flambaum, *Mon. Not. R. Astron. Soc.* **345**, 609 (2003).
5. J. K. Webb et al., *Phys. Rev. Lett.* **107**, 191101 (2011).
6. J. A. King et al., *Mon. Not. R. Astron. Soc.* **422**, 3370 (2012).
7. E. Reinhold et al., *Phys. Rev. Lett.* **96**, 151101 (2006).
8. A. Malec et al., *Mon. Not. R. Astron. Soc.* **403**, 1541 (2010).
9. F. van Weerdenburg, M. T. Murphy, A. L. Malec, L. Kaper, W. Ubachs, *Phys. Rev. Lett.* **106**, 180802 (2011).
10. J. van Veldhoven et al., *Eur. Phys. J. D* **31**, 337 (2004).
11. M. T. Murphy, V. V. Flambaum, S. Muller, C. Henkel, *Science* **320**, 1611 (2008).
12. C. Henkel et al., *Astron. Astrophys.* **500**, 725 (2009).
13. N. Kanekar, *Astrophys. J. Lett.* **728**, L12 (2011).
14. P. Jansen, L.-H. Xu, I. Kleiner, W. Ubachs, H. L. Bethlem, *Phys. Rev. Lett.* **106**, 100801 (2011).
15. S. A. Levshakov, M. G. Kozlov, D. Reimers, *Astrophys. J.* **738**, 26 (2011).
16. C. C. Lin, J. D. Swalen, *Rev. Mod. Phys.* **31**, 841 (1959).
17. P. Jansen, I. Kleiner, L.-H. Xu, W. Ubachs, H. L. Bethlem, *Phys. Rev. A* **84**, 062505 (2011).
18. F. J. Lovas, *J. Phys. Chem. Ref. Data* **33**, 177 (2004).
19. S. Muller et al., *Astron. Astrophys.* **535**, A103 (2011).
20. S. P. Ellingsen, M. A. Voronkov, S. L. Breen, J. E. J. Lovell, *Astrophys. J. Lett.* **747**, L7 (2012).
21. D. L. Jauncey et al., *Nature* **352**, 132 (1991).
22. C. Lidman et al., *Astrophys. J.* **514**, L57 (1999).
23. T. Wiklind, F. Combes, *Nature* **379**, 139 (1996).
24. Adopting a standard Λ-cosmology with $H_0 = 73$ km s^{-1} Mpc^{-1}, $\Omega_m = 0.28$, $\Omega_\Lambda = 0.72$.
25. J. N. Chengalur, A. G. de Bruyn, D. Narasimha, *Astron. Astrophys.* **343**, L79 (1999).
26. See supplementary materials on *Science* Online.
27. S. Muller, M. Guélin, *Astron. Astrophys.* **491**, 739 (2008).
28. Each line required a change of receiver, for which reason the time intervals could not be shorter.
29. K. M. Menten et al., *Astron. Astrophys.* **492**, 725 (2008).
30. S. Leurini et al., *Astron. Astrophys.* **422**, 573 (2004).
31. S. M. Breckenridge, S. G. Kukolich, *Astrophys. J.* **438**, 504 (1995).
32. J. E. M. Heuvel, A. Dymanus, *J. Mol. Spectrosc.* **45**, 282 (1973).
33. H. S. P. Müller, K. M. Menten, H. Mäder, *Astron. Astrophys.* **428**, 1019 (2004).